Journal of Structural Geology, Vol. 11, No. 3, pp. 307 to 316, 1989
Printed in Great Britain

0191-8141/89 $03.00 + 0.00

Displacement gradients on fault surfaces

JOHN J. WALSH and JUAN WATTERSON

Department of Earth Sciences, University of Liverpool, P.O. Box 147, Liverpool L69 3BX, U.K.

(*Received* 1 *June* 1987; *accepted in revised form* 23 *September* 1988)

Abstract—The maximum displacements and the dimensions of single faults are systematically related and the variation in displacement, from a maximum at the centre of a fault to zero at an elliptical tip-line loop, is described by a simple theoretically derived expression. These relationships are used to examine the theoretical ranges and distributions of rates of change of displacement on fault surfaces. The dimensions and maximum displacement of a fault can be estimated from a limited number of displacement gradient measurements. Estimates are further constrained by a knowledge of the effective shear modulus of the rocks containing a fault. An understanding of displacement gradients can be applied to problems commonly encountered in mining operations and in the interpretation and use of seismic reflection data, in addition to field problems.

A comparison of theoretical displacement gradients with measured displacement gradients from British Coalfield faults shows that (i) fault surface ellipticities are between 1.5 and 2.5 and (ii) gross displacement gradients, expressed as the ratio of maximum displacement/long axis radius of the fault ellipse, range from 0.02 to 0.002. The measured displacement gradients indicate that the shear moduli of the faulted rocks range from 3 to 11 GPa, which is within the known range for Coal Measure rocks.

Displacement gradients along an array of fault segments are similar to those of single faults. For analysis of displacement gradients it is necessary to sum the discontinuous and continuous components of displacement; in extreme cases all the displacement may be accommodated by continuous deformation.

INTRODUCTION

MOST faults are characterized by varying displacement and an understanding of the rates of change of displacement on fault surfaces optimizes the use which can be made of displacement data from a restricted part of a fault surface. In particular, displacements can be predicted on those parts of a fault for which there is little or no data, as is often required in mining operations or hydrocarbon exploration and development. Alternatively, interpretations of seismic data can be tested for geometric and kinematic validity.

Displacement on a single fault surface varies from a maximum at the centre to zero at the fault tip (Rippon 1985a, Barnett *et al.* 1987). In ideal cases, all contours of displacement are elliptical, including the zero displacement contour, and concentric about the point of maximum displacement as is shown in Fig. 1, which also shows the nomenclature used. A systematic non-linear relationship between the maximum displacement on a fault and the dimensions of the fault surface (Watterson 1986, Walsh & Watterson 1988a), yields displacement gradients for faults (maximum displacement/fault radius) which vary from *ca* 0.002 on small faults with maximum displacements of about 1 m, to *ca* 0.1 on thrusts with maximum displacements of *ca* 40 km. The displacement gradient is also influenced by the material properties, in particular the shear modulus, of the rocks containing the fault (Walsh & Watterson 1988a).

In this paper we examine the theoretical ranges and distributions of displacement gradients on elliptical fault surfaces, and assemble measurements of horizontal and down-dip displacement gradients from normal faults recorded on mine plans from British coalfields. Comparable data can often be obtained in the field, from maps or plans, or from seismic sections and our objective is to encourage the collection and quantitative application of commonly available information. A theoretical model is provided which will undoubtedly need modification to suit local circumstances but which nevertheless provides a framework within which data can be examined and put to practical use: such data can also be used to test or modify the model.

THEORETICAL DISPLACEMENT GRADIENTS

Displacement gradients (hereafter, gradients) measured over small parts of an ideal elliptical fault surface vary according to (i) the direction in which the gradient is measured on the fault surface, (ii) the displacement profile along the fault radius, i.e. the manner in which displacement reduces from a maximum to zero along the

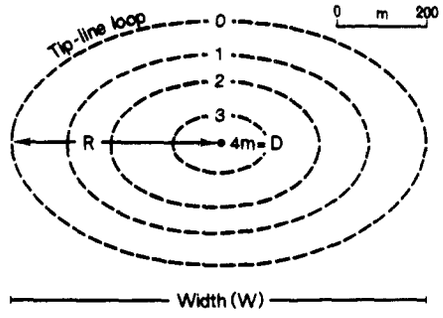

Fig. 1. Schematic diagram of elliptical fault surface bounded by a zero displacement contour (tip-line loop) with maximum displacement (D) in centre. Radius (R) and width (W) of the fault are also shown.

fault radius, (iii) the ellipticity of the fault surface, (iv) the mean gradient for the fault as a whole, i.e. the ratio maximum displacement/fault radius and (v) the distance over which a displacement change is measured (measuring interval). The effects of each of these factors on gradient values and distributions are considered below.

Direction of measurement

Only measurements of displacement gradient either parallel or normal to the displacement direction are considered; measurements made in other directions cannot be used.

Displacement profiles

The manner in which displacement reduces from a maximum to zero along a fault radius is expressed by a normalized displacement profile: this is a plot of displacement vs distance along the radius from the fault centre (Fig. 2), with both the maximum displacement and the length of the radius normalized to 1. The normalized displacement profile can be derived theoretically and is closely matched by data from actual faults recorded in British coalfields (Walsh & Watterson 1987). The theoretical displacement profile is derived from the elastic single slip event profile (Eshelby 1957) and a fault growth model (Watterson 1986).

The theoretical displacement gradients given below have been calculated using the expression for the theoretical normalized profile (Walsh & Watterson 1987)

$$d = 2(((1 + r)/2)^2 - r^2)^{1/2} (1 - r), \qquad (1)$$

where d = normalized displacement at a point on a fault surface and r = normalized radial distance from the fault centre.

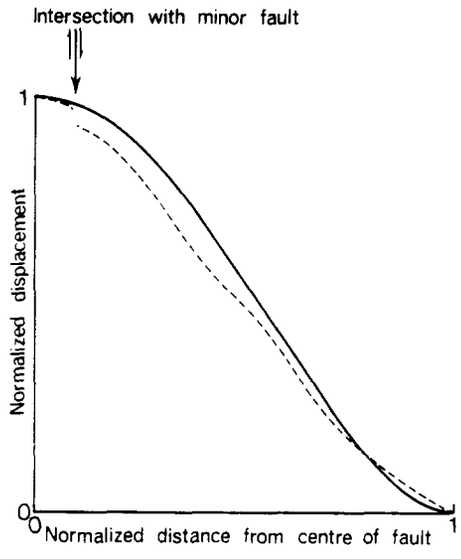

Fig. 2. Normalized displacement profiles along horizontal fault radii. Solid line—theoretical profile (Walsh & Watterson 1987). Broken line—profile for the Tiim Phonolites along the Saimo Fault, Kenya Rift Valley (Chapman *et al.* 1978). The position of a minor fault affecting this profile is shown.

The theoretical profile is shown in Fig. 2 together with the observed displacement profile of a fault from the Kenya Rift. The Rift fault has a radius of 28.6 km and maximum displacement of 3.4 km; the profile was constructed from a stratigraphic separation diagram illustrated in Chapman *et al.* (1978). As the displacement change is non-linear, a measurement of gradient made along a small section of a fault radius will differ from the mean gradient along the complete radius (Fig. 2).

Ellipticity of the fault surface

Normal faults in flat-lying sedimentary sequences have fault surface ellipses with horizontal major axes (Rippon 1985a,b, Barnett *et al.* 1987). If the elliptical form of the fault surface is due to the mechanical anisotropy of the sequence then different sequences might be characterized by different ellipticities, with circular faults possibly characteristic of mechanically isotropic rocks. If, on the other hand, elliptical fault surfaces are a product of the different energy requirements for propagation of screw and edge dislocations, elliptical faults will occur in mechanically isotropic rocks. This fundamental question has yet to be resolved. Ellipticities of well constrained coalfield faults (i.e. those for which there are sufficient data to contour displacements over the entire fault surface) range from 1.25 to 3.0 with a mean value of 2.25 (n = 20). Most of the theoretical gradient distributions illustrated in this paper are therefore calculated for fault surfaces with an ellipticity of 2.

Gross displacement gradients

Gross displacement gradient (G_g) refers to the mean displacement gradient (D/R) over the complete fault radius and is distinguished from the local gradient (G_l) values measured over smaller distances on a fault surface. On normal faults which have been contoured for displacement, and for which the fault surface ellipse is defined (Rippon 1985a, figs. 3 and 4, 1985b, figs. 5 and 6, Barnett *et al.* 1987, fig. 2), the horizontal axis is the major ellipse axis and therefore has a lower gross gradient than the down-dip axis. Gross gradients referred to here are those for horizontal radii, unless stated otherwise, because available data on lengths of fault radii in relation to maximum displacement are almost all for horizontal radii. An estimate of the gross gradient for a fault of maximum displacement (D) can be obtained as follows from the relationship (Walsh & Watterson 1988a)

$$D = W^2/P, \qquad (2)$$

where D = maximum fault displacement, W = maximum fault dimension (radius (R) = $W/2$) and P = variable related to rock properties. As the gross gradient, G_g = $2D/W$ then combining with (2)

$$G_g = 2D/(DP)^{1/2}$$
$$G_g = 2(D/P)^{1/2}$$

or $$G_g = k_D D^{1/2}, \qquad (3)$$

where $k_D = 2/P^{1/2}$.

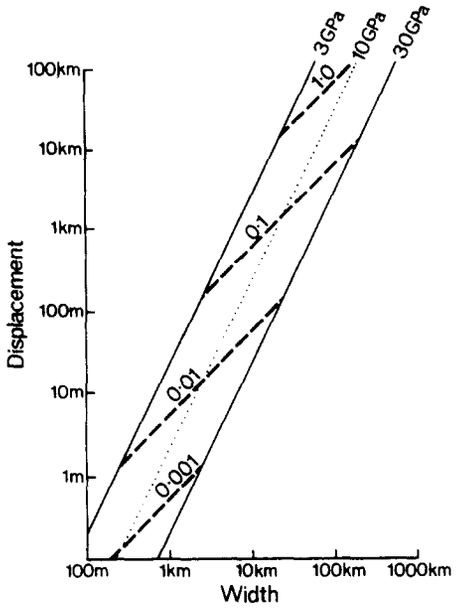

Fig. 3. Logarithmic plot of width vs maximum displacement showing bounding curves (solid) to fault data from Walsh & Watterson (1988a). Bounding curves are assigned shear modulus values of 3 and 30 GPa and the dotted curve represents a shear modulus value of 10 GPa (see text for details). Broken lines are contours of gross displacement gradient.

For rocks of low shear modulus (*ca* 3 GPa), e.g. hard shale, $P = 5 \times 10^4$ (see Walsh & Watterson 1988a, fig. 5) and $k_D = 0.009$. For sedimentary rocks of higher shear modulus (*ca* 10 GPa), e.g. hard sandstone, $P = 5 \times 10^5$ and $k_D = 0.003$. For metamorphic and igneous rocks, values of P range from 5×10^5 to 5×10^6 and k_D from 0.003 to 0.0009.

Alternatively, if the width (W) of a fault is known then

$$G_g = 2W/P$$

or

$$G_g = Wk_W \quad (4)$$

where $k_W = 2/P = k_D^2/2$ and corresponding values of k_W are 4×10^{-5}, 4×10^{-6} and 4×10^{-6} to 4×10^{-7}. The variation in fault displacement (D), fault width (W) and shear modulus is illustrated in Fig. 3. It is expected that the values quoted will need to be modified as more data become available.

Measuring interval

As with any non-linear function, displacement gradient values vary with the interval over which the gradient is measured. On a fault surface the gradient can be measured over a distance as large as the fault radius (it is then the gross gradient) or measured (as the local gradient) over successively smaller distances down to the vanishingly small. The smaller the measuring interval the greater the range of values obtained for a particular fault. Measuring intervals can be selected by one of three different criteria: (a) as a fixed proportion of the fault dimensions, (b) as a fixed multiple of the displacement at the point where the gradient is to be measured and (c) as the distance over which the displacement at the point to be measured changes by a fixed proportion. No criterion is more 'correct' than the others but a vanishingly small fixed interval corresponds most closely to usual mathematical convention of gradient: this method is used here to illustrate some of the systematics of gradient distribution and is the most suitable for comparison with the coalfield data. The second method has the disadvantage of not permitting meaningful comparisons between gradient distributions on faults of different size because gross gradients on large faults are much greater than on small faults. The third method, although *ad hoc*, has the advantage of corresponding most closely to the way in which measurements on faults can often be obtained in practice and can be adopted as a rule of thumb for measurements made in the field and from some other types of data: this method has been used to illustrate the gradient values and distributions against which real data can be compared.

THEORETICAL GRADIENT DISTRIBUTIONS

Measurement conventions

For normal faults the local gradient measured normal to the slip direction is referred to as the horizontal gradient (HG) and that measured parallel to the slip direction is referred to as the vertical gradient (VG), although it is in fact the down-dip direction and is not vertical.

Calculation of the gradient, G_l, at a point, p, at which the displacement is d, is illustrated in Fig. 4. The displacements at p_1 and p_2, which are equidistant from p, are d_1 and d_2 respectively. The distance between p_1 and p_2 is the measuring interval, MI, and $G_l = (d_1 - d_2)$ /MI. The measuring intervals for HG and VG will not be the same if the interval is defined by the criterion of proportional change of displacement. If p_2 lies outside the tip-line loop no gradient value is calculated. If the displacement at any point between p_1 and p_2 is higher than at either of those points, as would be the case if the line joining them intersected a principal axis of the ellipse, the convention is adopted that the position of p_1 is adjusted to lie on the principal axis: in such cases p_1 and p_2 are not equidistant from p. This convention avoids misleading values of zero gradient and allows a single quadrant of the ellipse to be used to represent the

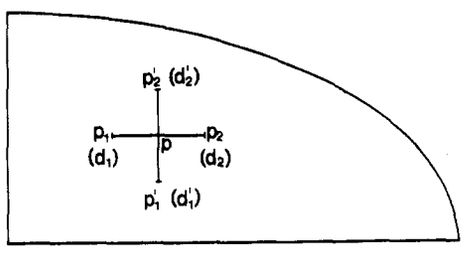

Fig. 4. Quadrant of fault surface ellipse (viewed normal to the fault surface) illustrating methods of calculation of theoretical gradient values at point p. For the example shown, the measuring interval (MI) for horizontal displacement gradient (HG) and vertical displacement gradient (VG) calculations is the same (i.e. the distance p_1 to p_2 or p_1' to p_2'). HG = $(d_1 - d_2)$/MI and VG = $(d_1' - d_2')$/MI. See text for details.

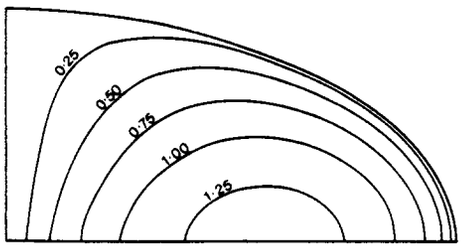

Fig. 5. Quadrant of fault surface ellipse (ellipticity = 2) showing contours of horizontal displacement gradient (HG) expressed as a fraction of the horizontal gross displacement gradient (0.01) appropriate to a fault in hard sandstone with D = 10 m. Measuring interval is 1% of the minor axis of the fault ellipse.

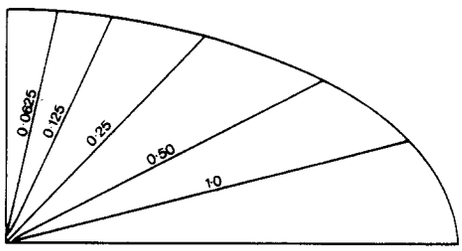

Fig. 7. Quadrant of fault surface ellipse (ellipticity = 2) showing contours of horizontal displacement gradient/vertical displacement gradient (HG/VG). Measuring interval is 1% of the minor axis of the fault ellipse.

whole fault surface: a gradient value is regarded as misleading if the displacement at a point between p_1 and p_2 is higher or lower than the displacement at both those points. Distributions are represented by measurements made on a square grid over a single quadrant of a fault surface ellipse with each measurement representing an equal area of the fault surface. Points on or near a principal axis of the fault ellipse are slightly over-represented in the distributions illustrated but this is of no significance for present purposes.

Spatial distribution of gradients

The displacement at any point on a fault surface can be calculated, using equation (1), for a fault of given maximum displacement, maximum dimension and ellipticity. Values of HG and VG at a point can then be obtained for a given measuring interval. The pattern of variation in HG values over a fault surface is illustrated by the contour pattern shown in Fig. 5. The fault ellipse has an axial ratio of 2 and the contour values shown are expressed as fractions of the gross horizontal gradient: a corresponding diagram for VG is shown in Fig. 6 and values are expressed as fractions of the vertical gross gradient. Elements of the two diagrams are compared in Fig. 7 in which contours are drawn for values of the HG/VG ratio: this ratio is always equal to the reciprocal of the fault ellipticity along a line equivalent to the zero extension direction of the ellipse. Changes of the gross displacement gradient and of measuring interval will alter the gradient values shown in Figs. 5 and 6 but will not change the overall pattern of variation.

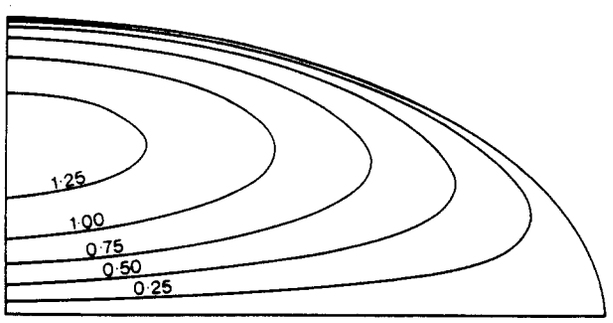

Fig. 6. Quadrant of a fault surface ellipse (ellipticity = 2) showing contours of vertical displacement gradient (VG) expressed as a fraction of the vertical gross displacement gradient of 0.01. Measuring interval is 1% of the minor axis of the fault ellipse.

Graphical representation of gradient values

A logarithmic plot of HG vs VG for a circular fault is shown in Fig. 8. The gross gradient of the fault is represented by the solid circle at the extremity of the concentration of calculated points. A change of gross gradient would simply displace the pattern along the line of symmetry of the data point distribution (Fig. 8). The range of values of local gradients derived for a single fault is almost two orders of magnitude and a single value of HG or VG constrains the size of the fault from which it is derived only within very broad limits. For example a single measurement on a 50 m outcrop over which displacement reduces from 10.5 m to 9.5 m (i.e. HG = 0.02) could represent a fault with a gross gradient anywhere between 0.015 and 0.75 because HG on the single fault shown in Fig. 8 varies by a factor of about 50, i.e. IV to VII. A single HG value only permits an estimation of fault width to within a factor of 50.

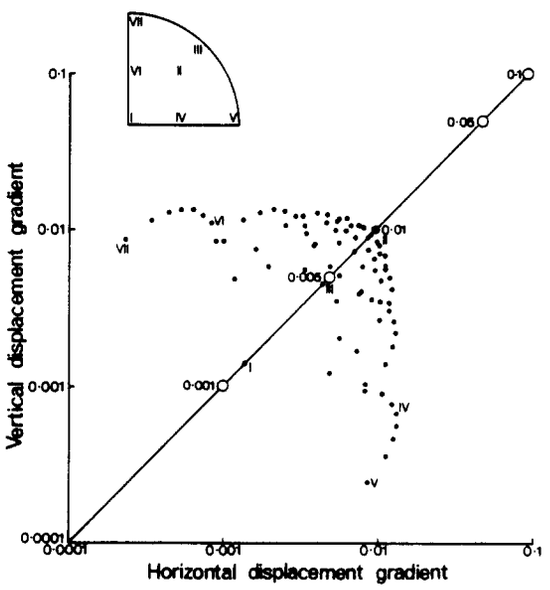

Fig. 8. Theoretical logarithmic plot of horizontal displacement gradient (HG) vs vertical displacement gradient (VG) for points on a circular fault surface (ellipticity = 1) with radius of 1 km and maximum displacement of 10 m. The fixed measuring interval is 10% of the fault radius. The solid circle defines the gross gradient (0.01) of this fault and the open circles show the corresponding points for faults with different gross gradients. Inset showing a single quadrant of the fault surface with the positions of plotted points numbered I–VII.

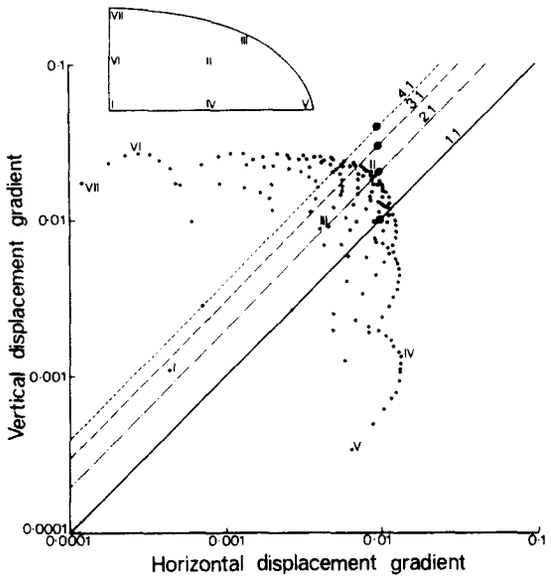

Fig. 9. Theoretical logarithmic plot of horizontal displacement gradient (HG) vs vertical displacement gradient (VG) for a fault surface (ellipticity = 2) with horizontal radius of 1 km and maximum displacement of 10 m. The measuring interval is 5% of the length of the minor axis of the fault ellipse. Symmetry lines for faults with ellipticities of 1, 2, 3 and 4 are also shown. The solid circles show the plotted positions for gross gradients on faults of varying ellipticity but of constant horizontal gross gradient (0.01). Inset shows a single quadrant of the fault surface ellipse with the positions of plotted points numbered I–VII.

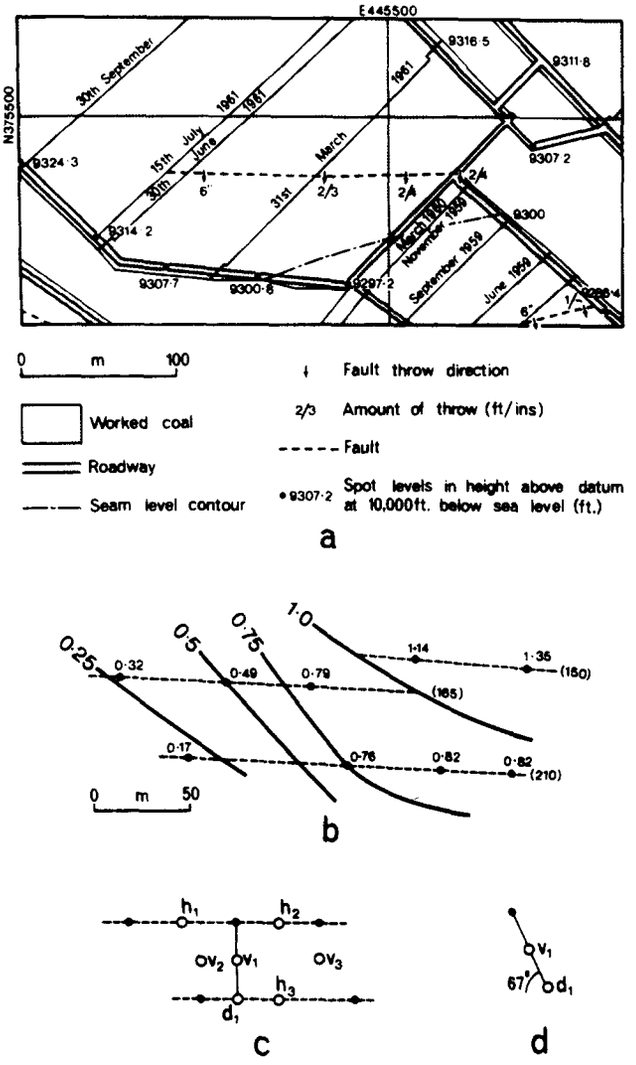

Fig. 10. (a) Part of standard mine plan SK/4475 for Deep Hard seam, Markham Colliery, North Derbyshire. National Grid co-ordinates are indicated. (b) Displacement contour diagram for fault shown in (a). The projection plane is vertical and strikes parallel to the Deep Hard fault trace. Displacements, in metres, are true displacement values, i.e. account has been taken of fault dip. Fault/seam intersections of worked coal seams are shown as dashed lines and levels (in brackets) are in metres below sea level. The Deep Hard fault/seam intersection, as shown in (a), is the lowest of the three fault/seam intersections. (c) Positions at which horizontal (h_i) and vertical (v_i) displacement gradients have been calculated for part of the fault shown in (b). Points at which displacement readings have been recorded are shown as solid circles. Horizontal displacement gradients are calculated at the mid-points between displacement readings on the same fault/seam intersection. Vertical displacement gradients are calculated at the mid-points between a displacement reading on one seam and an interpolated displacement value (e.g. d_1) on an adjacent seam. (d) Cross-section through fault shown in (c). Fault dip is accounted for in calculating the vertical displacement gradient between the recorded displacement reading (solid circle) and the interpolated displacement value (d_1).

The spread of points derived for a single fault is very much less when measured parallel to the line of symmetry; if the point derived from very close to the centre of the fault is ignored (point I, Fig. 8), the range in HG values is reduced to a factor of less than 4 (points II–III, Fig. 8). If values of both HG and VG are available for a single point the uncertainty is reduced to, what is for some purposes, a useful level. Values of 0.02 and 0.001 for HG and VG respectively would correspond to a fault with a gross gradient value between 0.015 and 0.067.

A change in the ellipticity of the fault surface displaces the distribution upwards parallel to the VG axis and also reduces the symmetry (Fig. 9). This figure shows the distribution of HG values for a fault surface with an ellipticity of 2 and also shows the lines of symmetry for ellipticities of 1, 2, 3 and 4.

Given a knowledge, or assumption, of the fault ellipticity, gradient measurements at a single point may allow a closer estimate of the fault dimensions. If the single plotted point falls on or near the appropriate symmetry line it will lie close to the point representing the gross gradient value for the fault, which can be estimated with high probability to within a factor of 2 (Fig. 9).

Where gradient data are available for only one direction on a fault surface a single gradient value is of little practical value. Where a large number of values are available some information can be derived from a frequency diagram or histogram, but more useful information can be derived from the gradient/displacement plot described later.

COALFIELD FAULT DATA

Data collection techniques

HG and VG values were measured on 74 faults, with maximum displacements of up to 10 m, which were identified as intersecting two or more worked seams (mean = 3.4) from mine plans (1:2500) of the East Pennine Coalfield (Fig. 10). We first constructed dip

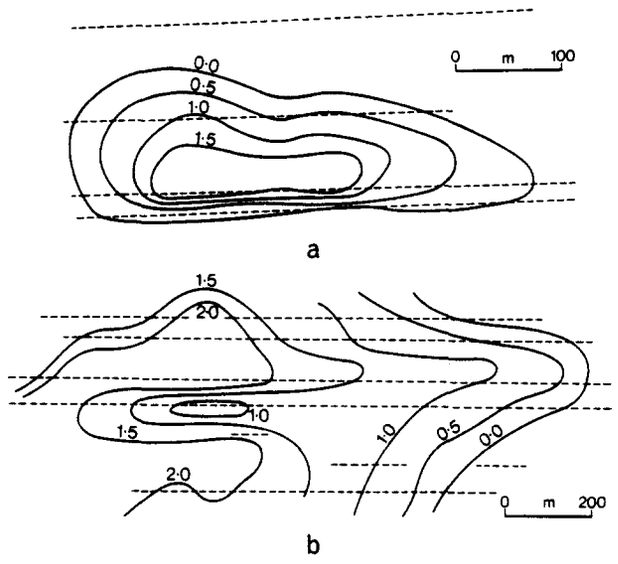

Fig. 11. (a) Displacement contour diagram for a fault from Markham Colliery, North Derbyshire. Displacement data are derived from worked coal seams, shown as dashed lines. Displacements contoured in metres. Redrawn from Rippon (1985a, fig. 3). (b) Partial displacement contour diagram for fault from Markham and Arkwright Collieries, North Derbyshire. Displacement data are derived from worked coal seams, shown as dashed lines. Redrawn from Rippon (1985a, fig. 6).

contour diagrams for each fault surface (see Rippon 1985a, figs. 3–9, Walsh & Watterson 1988b, fig. 4) and calculated true displacement values from the measured vertical displacement readings. Displacement contour diagrams (Fig. 11), showing the variation in displacement on a fault surface, were then constructed (Rippon 1985a, figs. 3–9, Barnett *et al.* 1987, fig. 2): the faults analysed were those for which displacement contours could be drawn for part of the fault surface (5–60%). Construction of displacement contour diagrams allowed sampling across principal axes of fault ellipses to be avoided. In cases where displacement was effected on more than one discrete fracture the displacement values were obtained by summing the displacements on overlapping segments (Fig. 12). Two measurements were made at selected points.

(i) Horizontal displacement gradient (HG): fault/seam intersections (fault traces on coal seam plans) have very low plunges and the gradients calculated between adjacent points on these traces were taken to be horizontal. The displacement halfway between adjacent recorded displacement readings was obtained by linear interpolation and HG measured from the two recorded readings (Fig. 10).

(ii) Vertical displacement gradient (VG): the gradient between fault/seam intersections on adjacent seams was calculated using a recorded displacement reading on one seam and an interpolated value on the other, upper or lower, seam. The calculation took account of the fault dip along the measuring interval. The displacement value mid-way between the two seams was obtained by linear interpolation (Fig. 10).

In many cases either the VG or the HG measurement was not made because of insufficient data. Where possible the measuring interval used for calculating HG spanned the same difference in displacement ($d_1 - d_2$) as that used for VG calculation at the same point. In most cases however, the displacement difference for the HG calculation was less than for the VG calculation because the VG measuring interval was effectively fixed by the

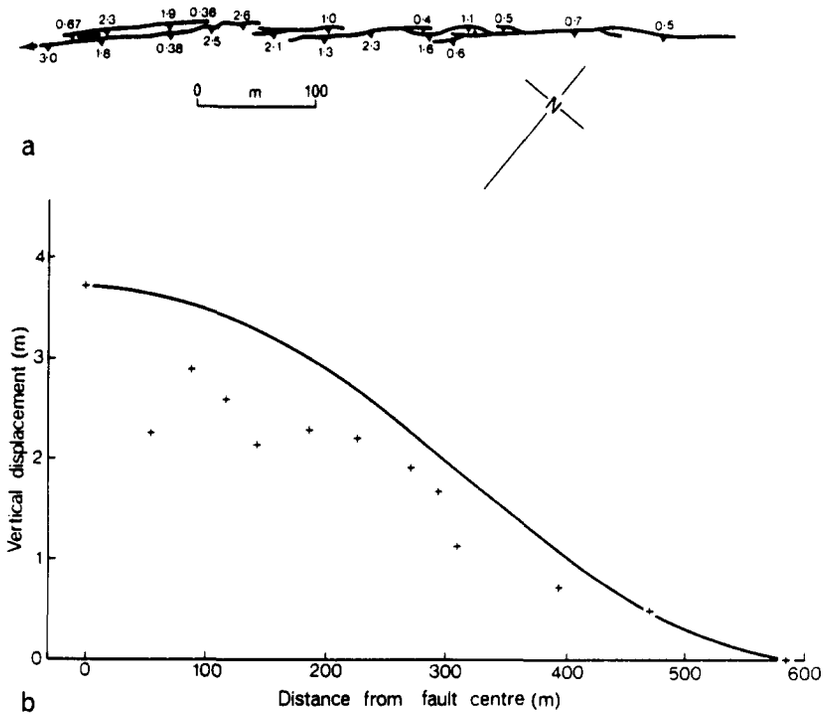

Fig. 12. (a) Fault/seam intersection on Top Hard seam, Welbeck Colliery, Nottinghamshire, with recorded vertical displacement values. (b) Displacement profile for the fault shown in (a). Zero displacement is taken as being 50 m beyond the mapped tip of the fault, for the reasons given in Walsh & Watterson (1987). The theoretical displacement profile for single faults is shown as a solid curve.

inter-seam stratigraphic thickness. Measuring intervals ranged between 10 and 250 m, as determined by the inter-seam thickness, with a mean of about 50 m. No gradient value was calculated where a reversal of gradient direction was apparent, i.e. across a principal axis of the fault ellipse.

Three combinations of HG, VG and displacement (d) data were collected:

(i) HG and d values were recorded at 1059 points on 63 faults;

(ii) VG and d values were recorded at 1069 points on 61 faults;

(iii) VG, HG and d values were recorded at 346 points on 51 faults.

To obtain an HG value at the same point as a VG reading (midway between two seams) further interpolation was required to obtain d_1 and d_2 (see Fig. 4), which was possible only if suitable displacement contours were available; as this was often not the case, points for which HG and VG were both available were much fewer than those where single HG or VG measurements were made.

The sampling points, which are controlled by data density, are taken to represent a random sample of the fault surfaces included in the analysis. The quality of data is affected by recording practices in the mines, because the ductile drag component of displacement is often not included in a displacement reading on a mine plan (Walsh & Watterson 1987). This practice effectively reduces the recorded displacement, and the reduction can sometimes be identified as an anomalous low on a displacement contour diagram (Fig. 11b). Where such anomalies were identified, a revised displacement contour diagram was constructed but it is likely that in some cases incorrect gradients have been processed. The data are also inadequate for low gradients: gradients of less than about 0.001 are under-represented because displacement readings are generally recorded to the nearest 0.1 m.

Coalfield gradient diagram

On an HG vs VG plot, coalfield displacement gradient measurements (Fig. 13) do not have a distribution similar to that shown in Figs. 8 and 9 because, unlike the theoretical distributions, the data derive from many faults of different sizes. When compared with the theoretical distributions shown in Figs. 8 and 9 the data are consistent with derivation from faults with gross gradients in the range 0.02–0.002. This accords with Walsh & Watterson (1988a) which established the range of gross gradients for coalfield faults examined as 0.029–0.0018 for 34 faults.

Figure 13 is of interest for the information it provides on the ellipticity of the coalfield faults studied. The line of symmetry for these data is defined by the 45° line on either side of which there is an equal number of data points. This corresponds to the line of symmetry for fault surfaces with an ellipticity of 1.8. Indeed, the ratio HG/VG of the mean values of HG (n = 1059) and VG (n = 1069) for the 74 faults studied is 1.71 and provides

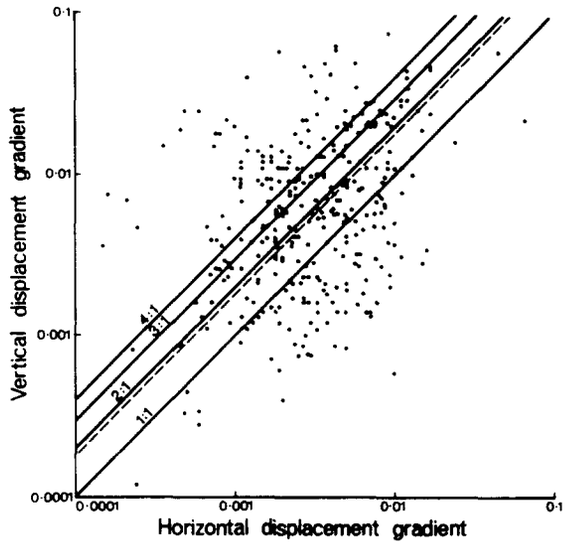

Fig. 13. Logarithmic plot of horizontal displacement gradient (HG) vs vertical displacement gradient (VG) for 346 points on 51 coalfield faults. Symmetry lines for fault ellipticities of 1, 2, 3 and 4 are shown as solid lines. Symmetry line for the 346 data points is shown by broken line (ellipticity = 1.8).

an additional though less accurate measure of coalfield fault ellipticity. These estimates compare with a mean ellipticity of 2.25 for the tip-line loops of complete contoured faults; none of these faults was used for measurement of gradient data. A value of 2 is regarded as a useful approximation for the ellipticity of faults of this size range in British coalfields, and this value has been used in calculating the gradient distributions which are given in the following section.

GRADIENT VS DISPLACEMENT PLOTS

Theoretical model

For the gradient to be measured at a point on a fault the displacement at that point must be known. A plot incorporating both gradient and displacement can provide a useful indication of the width and maximum displacement of a fault. Figures 14 and 15 are HG vs displacement (d) plots of points derived from a theoretical elliptical fault surface. In each diagram, data points derived from close to the minor axis of the fault ellipse are excluded because their gradients are usually lower than the minimum value of HG which might be measured in the field (<0.0005). The values plotted in Fig. 14 were obtained using a fixed measuring interval of 5% of the minor axis of the fault ellipse. The measuring interval used to derive the points plotted in Fig. 15 is the distance over which the displacement reduces by 5% from p_1 to p_2 (Fig. 4): this is the measuring interval criterion best suited to measurements in the field, where the fault dimensions are usually not known. For most practical purposes the displacement change can be taken as linear over this interval and the displacement at a point midway between p_1 and p_2 can be taken as the mean of the displacements at those points.

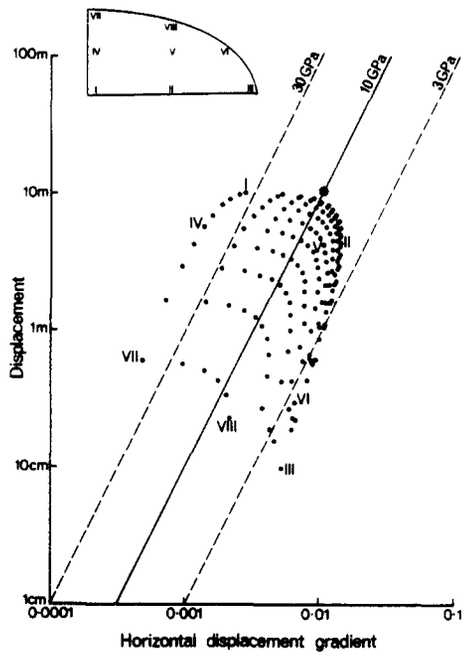

Fig. 14. Theoretical logarithmic plot of horizontal displacement gradient (HG) vs displacement (d) for points on a fault of horizontal radius 1 km, maximum displacement 10 m and an ellipticity of 2. Measuring interval is 50 m (i.e. 5% fault ellipse minor axis). Solid circle shows the position of the gross displacement gradient and maximum displacement of this fault. Solid line represents locus of all gross gradient and maximum displacement values for faults in rocks of shear modulus 10 GPa. Broken lines define the locus of faults in rocks of 3 and 30 GPa. Inset shows a single quadrant of the fault surface ellipse with the positions of plotted points numbered I–VIII.

The large solid circles on Figs. 14 and 15 represent the maximum displacement and the gross gradient of the fault. The distribution pattern of points is the same for faults of all sizes and is simply displaced along the solid line shown (corresponding to a shear modulus of 10 GPa). Lines appropriate to shear moduli of 3 and 30 GPa are also shown in Figs. 14 and 15.

A single measurement of displacement gradient, made either in the field or from a map or seismic section, may be plotted on Fig. 15 to give an estimate, with very wide limits, of the size of the fault on which the measurement is made. An outcrop length of 20 m in which the displacement changes from 50 to 40 cm would be consistent with a fault of maximum dimension between 200 m and 50 km. This estimate is of no practical value but if the rock type is of moderate shear modulus (10 GPa), the measurement would correspond to a fault of maximum dimension between 600 m and 6 km. It would clearly be imprudent to place much confidence in an estimate based on a single measurement.

Gradient vs displacement: coalfield fault data

An HG vs displacement (d) plot of 346 measurements on 51 coalfield faults is shown on Fig. 16: only those data points for which both HG and VG were available are plotted. The pattern characteristic of a single fault is not evident because the data were derived from faults of different size and possibly of different effective shear moduli. The data are consistent with derivation from faults of maximum displacement less than 10 m with a range of shear moduli between about 3 and 11.5 GPa. The plotted positions of several points, lying to the right of the 3 GPa curve in Fig. 13, are attributed to poor data

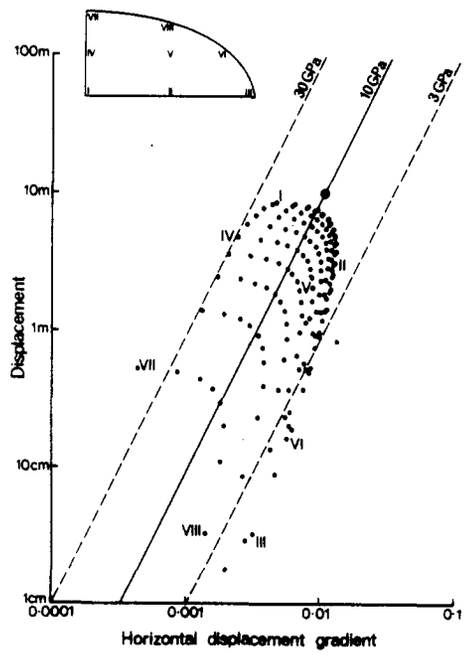

Fig. 15. Theoretical logarithmic plot of horizontal displacement gradient (HG) vs displacement (d) for same fault as shown in Fig. 14. Measuring interval is the interval over which the displacement changes by 5%. Solid circle shows the position of the gross displacement gradient and the maximum displacement of this fault. Lines representing the loci of faults in rocks of different shear moduli are those of Fig. 14. Inset as in Fig. 14.

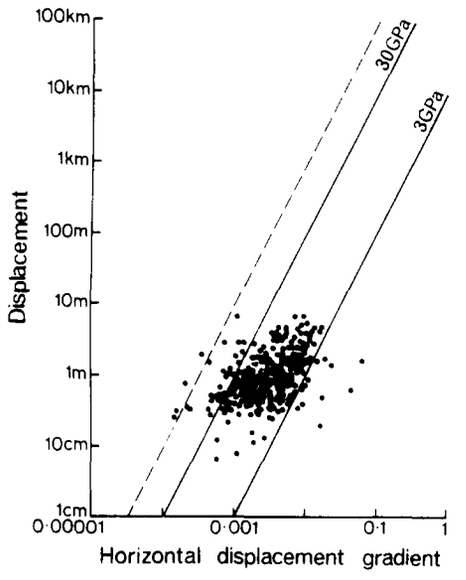

Fig. 16. Logarithmic plot of horizontal displacement gradient (HG) vs displacement (d) for 346 measurements derived from 51 faults in the East Pennine Coalfield. Solid lines are 3 and 30 GPa shear modulus curves as shown in Fig. 14. Broken line marks the limit of data points expected for faults with gross displacement gradients lying along the 30 GPa curve, using a fixed measuring interval.

due to variations in ductile drag giving anomalously high gradients (0.015–0.070) for displacements of less than 1.5 m.

VARIATIONS IN HG/VG RATIO ON GRADIENT VS DISPLACEMENT PLOT

The maximum information can be extracted from a gradient vs displacement plot if the HG/VG ratio (gradient ratio) at a point on the fault surface is known. The gradient ratio varies systematically within the field defined by the points derived from a single fault. As the variation and values of gradient ratio are independent of both fault size and gross gradient, the same pattern of gradient ratio contours can be used for all faults of a given ellipticity. The distribution pattern of values of gradient ratio do, however, vary with the method of determining the measurement interval. The simplest distribution pattern for gradient ratio values is derived from gradients measured with a fixed measuring interval, as shown in Fig. 17. This distribution is appropriate to a fault with an ellipticity of 2 and with gradients measured on a fixed interval equal to 5% of the minor ellipse axis; the distribution is not sensitive to the size of the fixed interval. Knowledge of the gradient ratio at a point enables the possible field for the fault to be much reduced and the significance of a single data point correspondingly increased. Because the contours of gradient ratio are sub-parallel to the displacement axis, a knowledge of the gradient ratio limits the possibilities more in terms of gross gradient and of shear modulus than in terms of maximum displacement. Figure 18 shows gradient ratio contours for the same fault but using a proportional rather than a fixed measuring interval; the contour pattern is more complex but the simplified version shown in Fig. 18 is the most appropriate for examination of gradient data from actual faults.

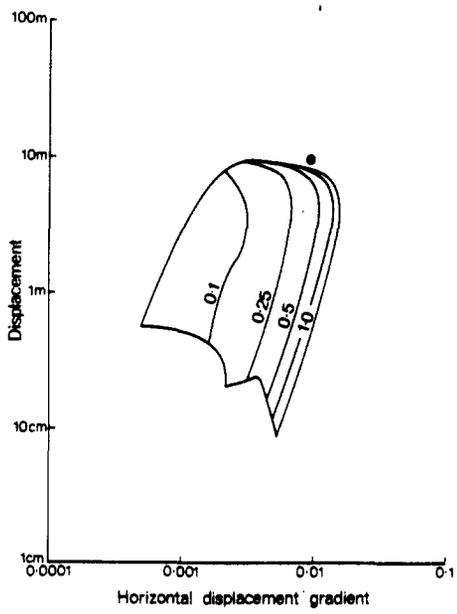

Fig. 17. Theoretical logarithmic plot of horizontal displacement gradient (HG) vs displacement (d) showing the boundary of the point distribution represented in Fig. 14 with contours of HG/VG ratios for the same fault (VG—slip-parallel displacement gradient). Solid circle represents the gross displacement gradient and maximum displacement for this fault.

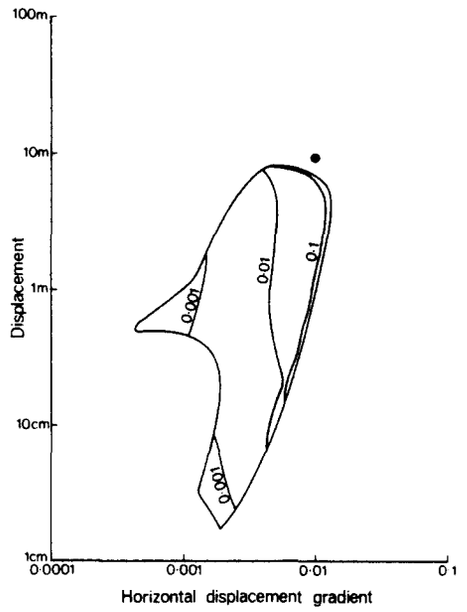

Fig. 18. Theoretical logarithmic plot of horizontal displacement gradient (HG) vs displacement (d) showing the boundary of the point distribution represented in Fig. 15 with contours of HG/VG ratios for the same fault (VG—slip-parallel displacement gradient). Solid circle represents the gross displacement gradient and maximum displacement for this fault.

DISCUSSION

The gradient values discussed are valid only for single faults from which there is no transfer of displacement onto nearby faults. Much higher displacement gradients occur locally near the tips of fault traces where individual traces form part of an array of overlapping faults, as shown in Fig. 12(a). In such arrays the individual traces are not independent structures, and have displacement characteristics different from those of single faults. Nevertheless, if the displacements on overlapping segments of an array are added together and the array is treated as a single fault, the systematics are comparable with those of a single fault (Fig. 12b). Detailed comparison of displacements along the fault (Fig. 12a) with those of a single fault is not possible because, (i) an accurate estimate of aggregate displacement is difficult due to the irregular distribution of displacement readings combined with the high and variable displacement gradients on overlapping segments and (ii) the displacement measurements are believed to exclude the continuous component of displacement (Walsh & Watterson 1987). It is likely that faults, if mapped on a sufficiently small scale, rarely consist of a single fault surface.

The systematic relationships described are those of an ideal model in which rock properties are uniform and can only be applied to the extent that the rocks containing a fault approach this ideal. While small faults may be contained entirely within a single lithology, this is not

the case for most faults in sedimentary successions. The dimensions of many faults are large compared with the scale of lithological variation and in such cases the relevant material properties can be taken to be those of the succession as a whole. However, in flat-lying successions the major axis of the fault ellipse may lie within a single lithology even though the fault surface as a whole may intersect several lithologies: it is likely that this is the lithology in which the fault nucleated. In such cases the fault width (Fig. 1) may be controlled by the properties of this single lithology and the fault surface may be an irregular ellipse with relatively greater dimensions in layers of higher shear modulus and relatively smaller dimensions in layers of low shear modulus. This feature is a problem only if the fault displacement is regarded as confined to that across a discontinuity. In practice, displacement of some layers may be partly or wholly accommodated by folding, i.e. normal drag. For analysis of displacements it is necessary to sum the discontinuous and continuous components: in extreme cases all the displacement may be accommodated by ductile deformation without the development of a discontinuity surface, as in a ductile shear zone. It is not uncommon in sedimentary sequences for faults to be discontinuities in more competent lithologies but with no discontinuity developed in less competent layers. This feature may affect the apparent ellipticity of a fault if the discontinuity dies out upwards or downwards at the boundary of an incompetent layer and the fault is regarded as terminating at this boundary (Fig. 11a). As pointed out by Rippon (1985b), a reduction in discontinuous displacement may also be observed towards the centres of faults along those coal seams in which a high proportion of displacement is characteristically accommodated by ductile drag (Fig. 11b). These features are due less to the properties of the coal seam itself, which is fairly competent, than to it being bounded on both sides by thick and very soft clays.

Displacement gradients on synsedimentary faults which have been derived from measurements of displacement on syn-faulting layers are influenced by additional factors: (i) the displacement/width characteristics for faults intersecting these layers are significantly different from those which characterize the fault as a whole (Walsh & Watterson 1988a) and (ii) changes in the rate of fault displacement produce complementary changes of vertical (slip-parallel) displacement gradients.

CONCLUSIONS

(1) The ellipticities of coalfield normal faults range from 1.25 to 3, with a mean value of about 2.

(2) Values of both horizontal and vertical (slip-parallel) displacement gradients (HG and VG) for a single point on a fault may be used to estimate the gross displacement gradient (i.e. the ratio maximum displacement/radius) of a fault to within a factor of 4, in favourable circumstances.

(3) Assuming a value of fault ellipticity, an HG vs VG plot of displacement gradient data from a single point on a fault may permit estimation of the gross displacement gradient of the fault to within a factor of 2.

(4) Given a knowledge of the effective shear modulus of the rocks containing a fault, values of HG and of displacement at a single point on a fault may be used to estimate the maximum dimension of the fault only to within one order of magnitude.

(5) An HG vs displacement diagram with contoured values of HG/VG ratio may be used to provide a more precise estimate of the dimensions and maximum displacement of a fault.

(6) High displacement gradients occur on overlapping segments of a fault. If the displacements on overlapping segments are added together and the array treated as a single fault, the displacement gradients are comparable with those of a single fault.

(7) Displacement may be partly or wholly accommodated by ductile deformation (ductile drag). The proportion of discontinuous to continuous (ductile) displacement depends on the mechanical properties of the faulted rocks and will therefore vary over a fault surface intersecting a multilayer sequence.

Acknowledgements—We thank John Mortimer and Iwan Williams for their assistance in data collection from coalmine plans. Several improvements are due to a review by Jim Evans. The work was funded by British Coal and the European Coal and Steel Commission (contract Nos YCE. 30/19572 & YCE. 30/20214), the U.S. Earthquake Hazards Reduction Program (contract No. 14-08-0001-22072) and the Natural Environment Research Council (grant GR3/4719). This paper is published with the permission of British Coal, but the views expressed are those of the authors and not necessarily those of British Coal.

REFERENCES

Barnett, J. A. M., Mortimer, J., Rippon, J. H., Walsh, J. J., Watterson, J. 1987. Displacement geometry in the volume containing a single normal fault. *Bull. Ass. Petrol. Geol.* **71**, 925–937.

Chapman, G. R., Lippard, S. J. & Martyn, J. E. 1978. The stratigraphy and structure of the Kamasia Range, Kenya Rift Valley. *J. geol. Soc. Lond.* **135**, 265–281.

Eshelby, J. D. 1957. The determination of the elastic field of an ellipsoidal inclusion and related problems. *Phil. Trans. R. Soc. Lond.* **A241**, 376–396.

Rippon, J. 1985a. Contoured patterns of the throw and hade of normal faults in the Coal Measures (Westphalian) of north-east Derbyshire. *Proc. Yorks. geol. Soc.* **45**, 147–161.

Rippon, J. 1985b. New methods of forecasting the throw and hade of faults in some North Derbyshire Collieries. *Trans. Inst. Min. Engrs*, 198–204.

Walsh, J. J. & Watterson, J. 1987. Distribution of cumulative displacement and of seismic slip on a single normal fault surface. *J. Struct. Geol.* **9**, 1039–1046.

Walsh, J. J. & Watterson, J. 1988a. Analysis of the relationship between displacements and dimensions of faults. *J. Struct. Geol.* **10**, 239–247.

Walsh, J. J. & Watterson, J. 1988b. Dips of normal faults in British Coal Measures and other sedimentary sequences. *J. geol. Soc. Lond.* **145**, 859–873.

Watterson, J. 1986. Fault dimensions, displacements and growth. *Pure & Appl. Geophys.* **124**, 365–373.